

Supporting Information for:

Native Electron Capture Dissociation Maps to Iron-Binding Channels in Horse Spleen Ferritin

Owen S. Skinner^{†‡*}, Michael O. McAnally^{†‡}, Richard P. Van Duyne[†], George C. Schatz[†],
Kathrin Breuker[§], Philip D. Compton[†] and Neil L. Kelleher^{†*}

[†] Department of Chemistry, Northwestern University, Evanston IL, USA

[§] Institute of Organic Chemistry, University of Innsbruck, Innsbruck, AUSTRIA.

Table of Contents:

Figure S-1. Fragment map of CAD from the 14+ ejected ferritin L-chain.

Figure S-2. Fragment map of activation of gas-phase isolated ferritin complex.

Figure S-3. Experimental setup of FIRE.

Figure S-4. FIRE-driven NECD fragments of cytochrome *c*.

Figure S-5. Experimental setup and fragment map of FIRE distance dependence.

Figure S-6. Experimental setup and mass spectra of FIRE with a misaligned laser.

Figure S-7. Fragment map of ferritin NECD driven by FIRE.

Figure S-8. Fragment map of NECD from the apoferritin L-chain.

Table S-1. Masses and errors for the matched fragment ions displayed in fragment maps:
“Supp_Table_1.xlsx”.

N S S Q I R Q N Y | S T E | V E | A A V N R | L | V | N | L | Y L R 25
 26 A | S | Y | T Y L S | L G | F | Y F D | R | D | D | V A L | E | G V | C H F 50
 51 F R E L A E | E K R E G A E R L L K M Q N Q R G G R 75
 76 A L F Q | D | L Q K | P S Q D | E | W G T T L D | A | M | K A | A I 100
 101 | V | L | E | K S L N Q A L L D | L H A L | G S A Q A D | P | H | L 125
 126 | C | D | F L E | S | H | F | L | D | E | E | V | K | L | I | K | K | M | G | D | H L T N 150
 151 I Q R | L V | G S Q | A | G L G E Y L F | E R L T L K H D C

Figure S-1. Graphical fragment map representation of fragment ions formed from quadrupole-based isolation and CAD dissociation of the 14+ L-chain ejected from the intact ferritin complex. Only *b*- and *y*-type fragment ions were detected. The red square corresponds to an N-terminal acetylation modification and the orange square corresponds to a cysteine methyl disulfide modification.

N S S Q I R Q N Y S T E V E A A V N R L V N L Y L | R 25
 26 A S Y T Y | L S L G F Y F D R | D D V | A | L | E | G V | C H F 50
 51 F R | E L A E E K R E G A E R L L K M Q N Q R G G R 75
 76 A L F Q D L Q K P S Q D E W G T T L D A M K A A I 100
 101 V L E K S L N Q A L L D L H A L G S A Q A D P H L 125
 126 C D F L E S H F L D E E V K L I K K M G D H L T N 150
 151 I Q R L V G S Q A G L G E Y L F E R L T L K H D C

Figure S-2. Evidence of NECD *c*-fragment ions from the L-chain obtained from quadrupole-based isolation and activation of the intact ferritin complex. These product ions must therefore be formed after quadrupole isolation.

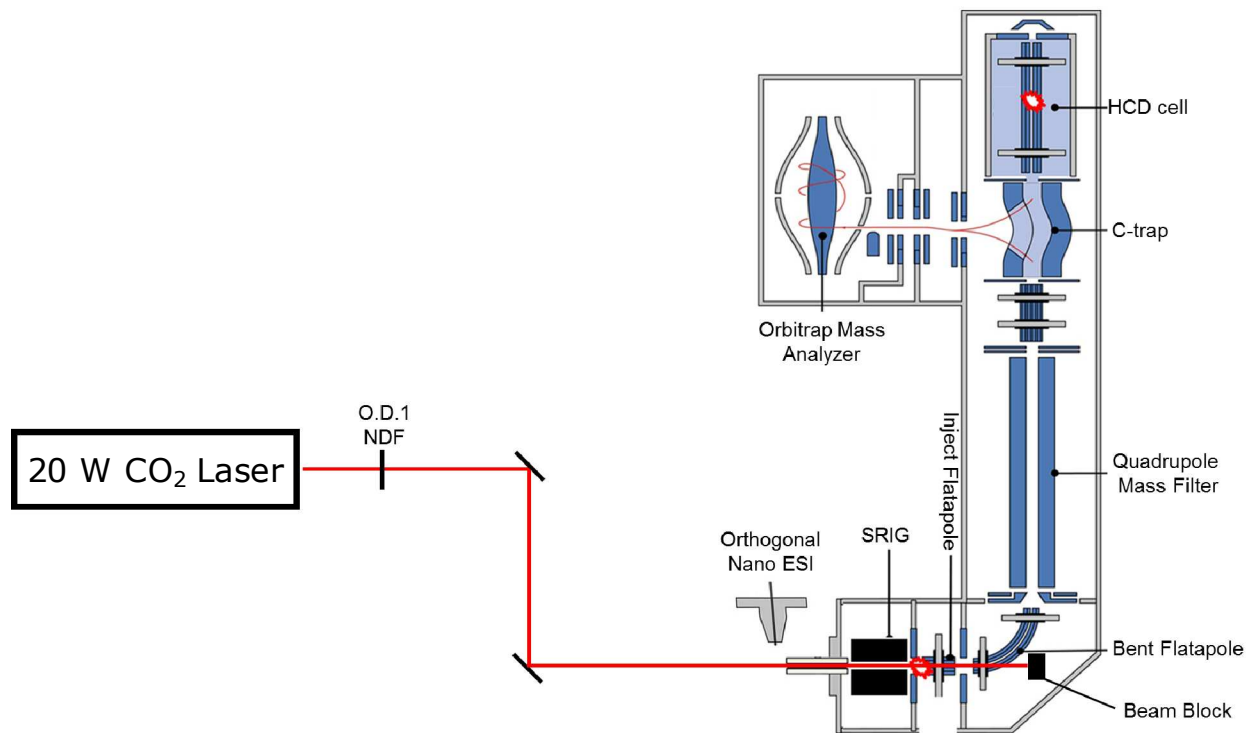


Figure S-3. Experimental setup for front-end infrared excitation (FIRE). The laser is aligned collinearly through the inlet capillary of the instrument, and blocked by a beam block placed behind the bent flatapole. The MS-portion of this figure was modified from Ref. 6.

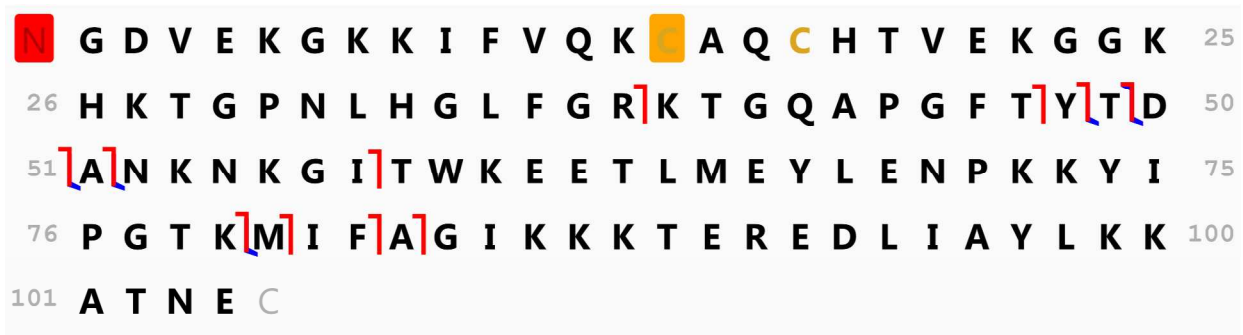


Figure S-4. Fragment map showing the NECD *c*- and complementary *y*-type cleavage products of cytochrome *c* upon laser activation by FIRE. The orange box corresponds to the mass shift caused by the covalent heme binding (+615.1695 Da), which is also bound to Cys-17. No fragment ions were observed without laser activation (data not shown).

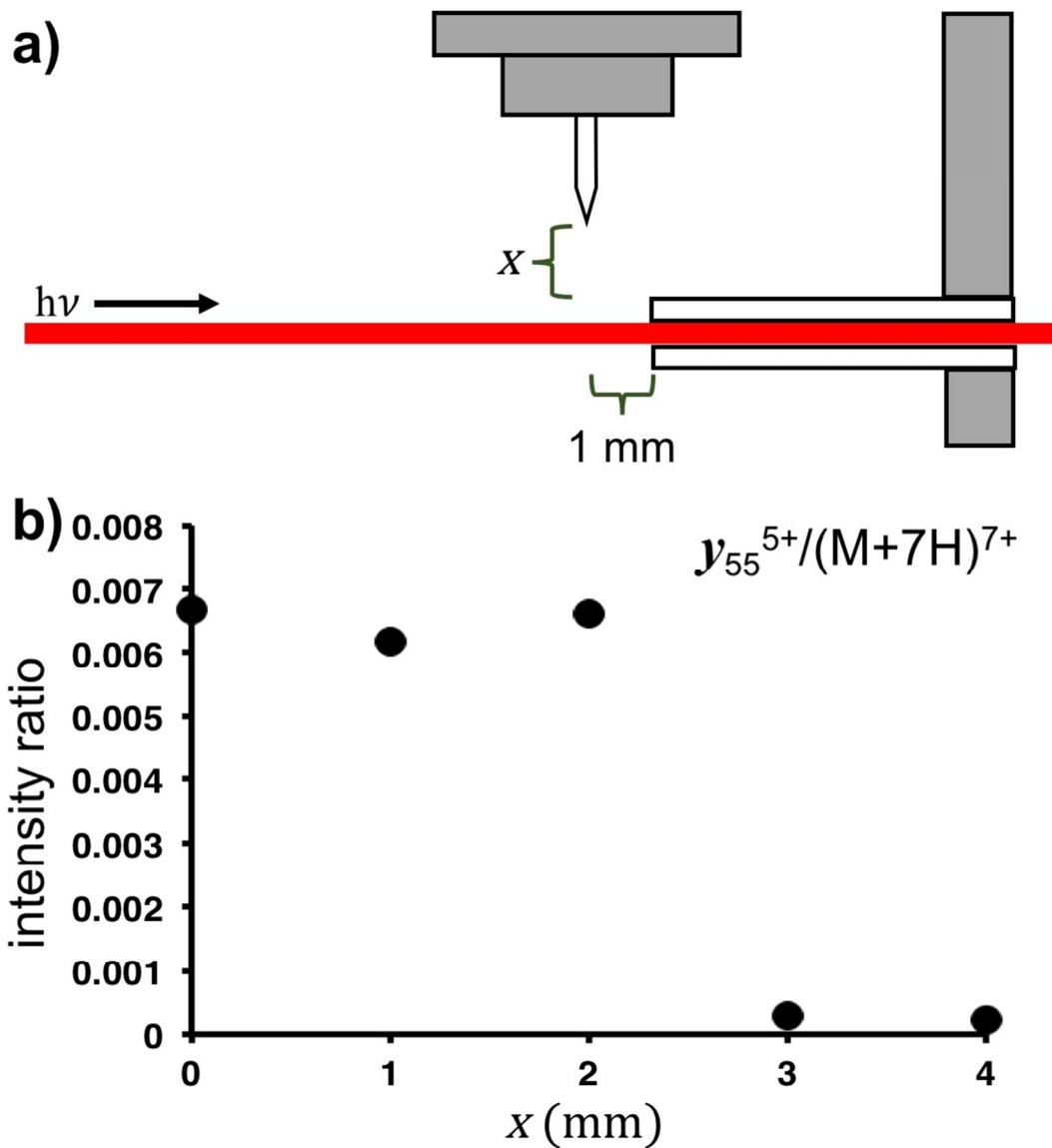


Figure S-5. (a) Experimental schematic of the FIRE setup highlighting the distance parameters used; x is the variable tip-laser distance. (b) The relative ratio of the y_{55}^{5+} compared to the $7+$ molecular ion of cytochrome c at varying electrospray emitter distances. The y_{55} fragment is an abundant NECD product ion and its intensity after normalization to the molecular ion is used to indicate the extent of NECD cleavage.

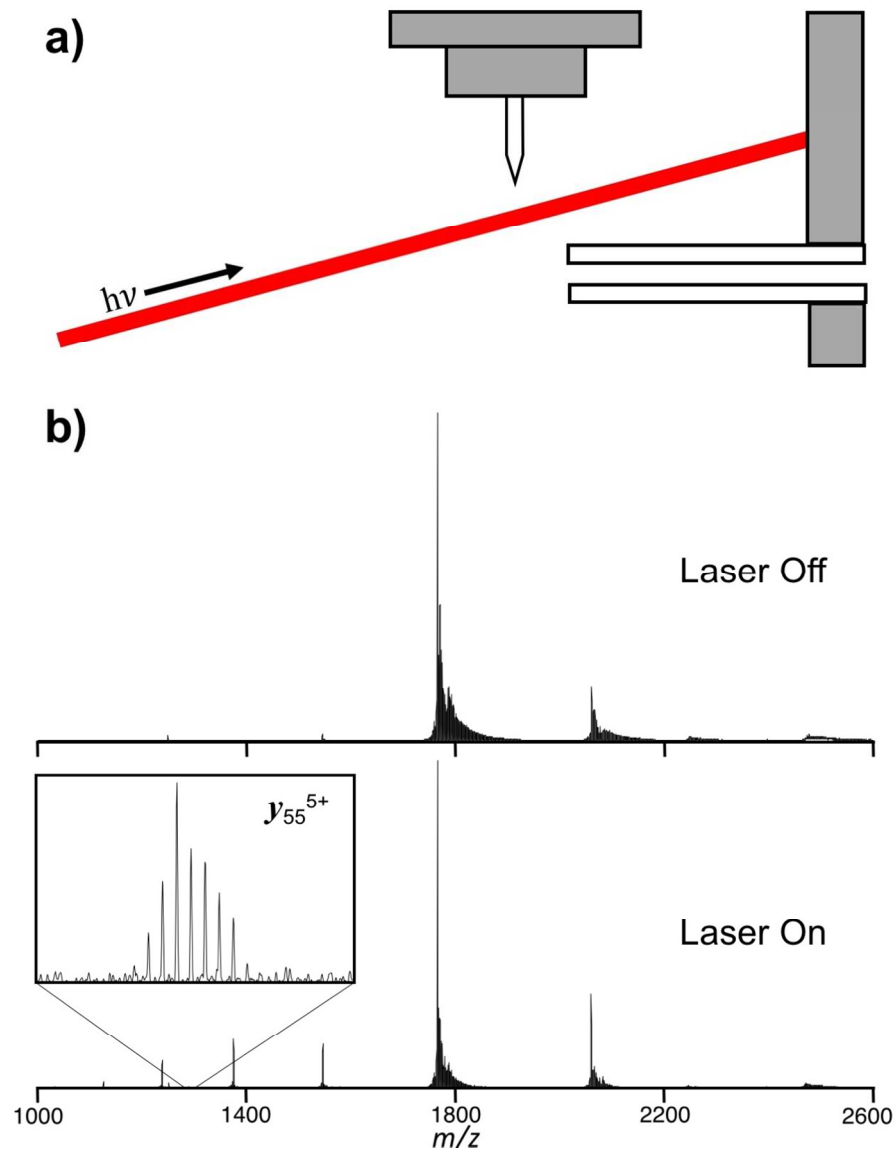


Figure S-6. (a) Experimental schematic of the intentionally misaligned FIRE setup. (b) Spectra of cytochrome *c* with the laser off (top) and on (bottom). Laser irradiation with FIRE produced evidence of higher-charged monomers and NECD fragmentation, despite only overlapping with the sample just after exit from the electrospray tip. Thus, the majority of ion activation from FIRE occurs in the droplet.

N S S Q I R Q N Y S T E V E A A V N R L V N L Y L R 25
 26 A S Y T Y L S L G F Y F D R D D V A L E G V C H F 50
 51 F R E L A E E K R E G A E R L L K M Q N Q R G G R 75
 76 A L F Q D L Q K P S Q D E W G T T L D A M K A A I 100
 101 V L E K S L N Q A L L D L H A L G S A Q A D P H L 125
 126 C D F L E S H F L D E E V K L I K K M G D H L T N 150
 151 I Q R L V G S Q A G L G E Y L F E R L T L K H D C

Figure S-7. Fragment map of ferritin activated by FIRE exhibiting *c*-fragment ions.

N S S Q I R Q N Y S T E V E A A V N R L V N L Y L R 25
 26 A S Y T Y L S L G F Y F D R D D V A L E G V C H F 50
 51 F R E L A E E K R E G A E R L L K M Q N Q R G G R 75
 76 A L F Q D L Q K P S Q D E W G T T L D A M K A A I 100
 101 V L E K S L N Q A L L D L H A L G S A Q A D P H L 125
 126 C D F L E S H F L D E E V K L I K K M G D H L T N 150
 151 I Q R L V G S Q A G L G E Y L F E R L T L K H D C

Figure S-8. Activation of the apo-form of horse spleen ferritin produced similar *c*-fragments to the holo-form, suggesting that the iron mineral core is not implicated in NECD.